

# An Experimental Comparison of Sliding Mode and Immersion and Invariance Adaptive Controllers for Position-feedback Tracking of a Simple Mechanical System with Friction

Luis Cervantes-Pérez <sup>a</sup>, Víctor Santibáñez <sup>a</sup>, Jesús Sandoval <sup>b</sup>, Romeo Ortega <sup>c</sup>,  
Jose Guadalupe Romero <sup>c</sup>,

<sup>a</sup> *Tecnológico Nacional de México / I.T. de La Laguna, Blvd. Revolución y, Av. Instituto Tecnológico de La Laguna s/n, Torreón, Coahuila, México, 27000.*

<sup>b</sup> *Tecnológico Nacional de México / I.T. de La Paz, Blvd. Forjadores de Baja California Sur 4720, La Paz, Baja California Sur, México, 23080.*

<sup>c</sup> *Departamento de Ingeniería Eléctrica y Electrónica / I.T. Autónomo de México, Río Hondo 1, CDMX, México, 01080.*

---

## Abstract

The purpose of this paper is to illustrate, in an experimental facility consisting of a simple pendular device, the performance of a sliding mode adaptive position-feedback tracking controller of mechanical systems with friction reported in the literature. To put this experimental evidence in perspective, we compare the performance of the sliding mode scheme with the one obtained by an adaptive controller designed following the well-known immersion and invariance technique.

*Key words:* Nonlinear Friction, Adaptive Observers, Tracking Control

---

## 1 Introduction

It is widely accepted in the control community that it is undesirable to differentiate signals and to inject high-gain (HG) in a control loop. It is well-known that both actions have the deleterious effects of reduction of the stability margins and noise amplification, the latter being unavoidable in any practical application, in particular, in mechanical systems. Both operations are intrinsic to sliding mode (SM) designs, that have proliferated in the theoretical control literature in the last few years.

A critical discussion on the “*sui géneris*” control theoretic scenario adopted for the application of some SM designs is carried out in Ortega, Romero & Fang 2025. Namely, the system dynamics is rewritten as the cascade

connection of a very simple part—usually a linear time invariant plant with known parameters—which is “perturbed” by an additive “*disturbance*” that is assumed to satisfy some Lipschitz-like condition. The latter assumption allows the designer to propose a HG mechanism, *e.g.*, an infinite gain relay operator, that “*dominates*” the “*disturbance*”. To accomplish the latter task, it is assumed that the signals are *bounded*, invoking the specious assumption that the system lives in some compact set. It is argued in Ortega, Romero & Fang 2025 that, neither the assumed scenario nor the standing assumptions, are compatible with current engineering practice in a large variety of applications. Experimental evidence of the aforementioned deleterious effects of HG injection were reported over forty years ago in Ortega 1982, and more recently in Aranovskiy, Ortega, Romero & Sokolov 2019.

Our objective in this paper is to bring again to the readers attention these facts. This time we illustrate it with an experimental facility consisting of a simple pendular device, for which we implement a SM adaptive position-feedback tracking controller of mechanical systems with friction reported in Davila, Fridman & Poznyak 2006. To

---

*Email addresses:* d.lecervantesp@lalaguna.tecnm.mx (Luis Cervantes-Pérez),  
vasantibanezd@lalaguna.tecnm.mx (Víctor Santibáñez),  
jesus.sg@lapaz.tecnm.mx (Jesús Sandoval),  
romeo.ortega@itam.mx (Romeo Ortega),  
jose.romerovelazquez@itam.mx (Jose Guadalupe Romero).

put this experimental evidence in perspective, we compare the performance of the SM scheme with the one obtained by the adaptive controller reported in Romero, Ortega, Fang & Bobtsov 2025, which is designed following the well-known immersion and invariance (I&I) technique Astolfi, Karagiannis & Ortega 2008.

The remainder of our paper is organized as follows. In Section 2 we describe the experimental facility and explain the tasks that we wish to accomplish. In Section 3 we present the speed observers and adaptive controllers to be tested experimentally. Sections 4 and 5 are devoted to the presentation of the experimental results, for the speed observation and trajectory tracking tasks, respectively. A final set of comparative simulation results on a hydro-mechanical system reported in Estrada, Ruderman, Texis-Loaiza & Fridman 2025 for the SM design and in Romero, Ortega, Fang & Bobtsov 2025 for an I&I one is presented in Section 6. We wrap-up the paper with some concluding remarks in Section 7.

## 2 Description of the Experimental Facility and Tests

### 2.1 Experimental set up

We consider in this paper the pendular device depicted in Fig. 1, consisting of a direct-drive arm with a single vertical link.

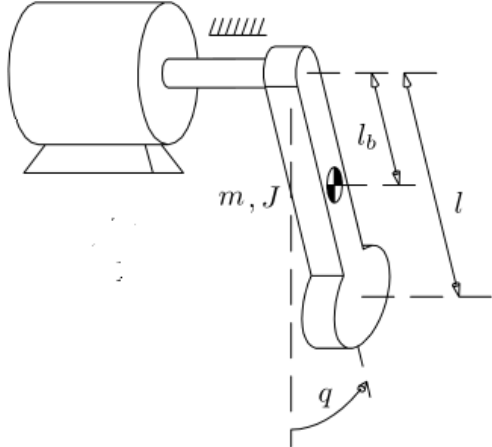


Fig. 1. Sketch of the pendular device.

We assume that the device is subject to a friction force, whose behavior is approximated by Coulomb and static friction Armstrong-Hélouvy, Dupont & De Wit 1994.

This leads to the following well-known dynamic model of the pendular device

$$J\ddot{q} + \theta_1\dot{q} + \theta_2 \tanh(\vartheta\dot{q}) + ml_b g \sin(q) = u, \quad (1)$$

where  $q(t) \in [0, 2\pi]$  is the pendulum angle,  $u(t) \in \mathbb{R}$  is the input torque,  $\theta_1 > 0$  is the viscous friction coefficient,  $\theta_2 > 0$  is a Coulomb friction coefficient, whose relay model is approximated with a  $\tanh(\cdot)$  function—with  $\vartheta > 0$  a large number—and the positive constants  $J, m, g$  and  $l_b$  are physical parameters, as depicted in Fig. 1, which are assumed to be *known*. To simplify the notation we define  $x_1 := q$  and  $x_2 := \dot{q}$ .

The experimental device was designed and built at the La Laguna Technological Institute, Mexico. A picture of the pendular device is shown in Fig. 2.



Fig. 2. Pendular device.

The joint is actuated by a direct-drive DC motor manufactured by Yokogawa Electric Corporation, model *DM1A200G*. The motor operates in torque mode, providing a maximum torque of  $\pm 200$  [Nm]. It is also equipped with a high precision relative encoder offering a resolution of 1,024,000 pulses per revolution. The proposed controller was implemented digitally in MATLAB using the Simulink Desktop Real-Time environment, with a sampling period of 1 [ms]. The experiments were conducted on a PC running Windows 10, equipped with an *Intel Core i5-14600K* CPU, 32 GB of RAM, an RTX 3060 GPU, and a 512 GB M.2 SSD. Communication between the PC and the robot was established through a Sensoray 626 data acquisition card (DAQ) installed in the PCI port of the motherboard. The DAQ interfaced with the motor driver (PARKER COM-PUMOTOR model DMG3-1200A) by sending analog voltage signals corresponding to the control torques. In turn, the driver transmitted pulse trains replicating the motor encoder signals to the DAQ digital inputs.

The physical parameters of the link are listed in Table 1, and they were originally reported in Gamez-Herrera, Sifuentes-Mijares, Santibañez & Gendarilla 2025; Gan-

darilla, Santibáñez, Sandoval & Campa 2022. The table summarizes the meaning of the parameters and their numerical values. The number  $\vartheta$  was changed in the various experiments, and is given in the corresponding sections.

## 2.2 Experimental tests

We tried experimentally two speed observers and associated adaptive tracking controllers:

- (i) the one based on I&I recently reported in Romero, Ortega, Fang & Bobtsov 2025;
- (ii) the SM scheme described in Davila, Fridman & Poznyak 2006.

For these two schemes we carried-out the following experimental tests.

**T1** Open-loop test of the observers for two different input signals:

$$u(t) = \begin{cases} 25 \sin(5t) \\ 14 \operatorname{sign}(\sin(\frac{\pi t}{3})) \end{cases}.$$

**T2** Adaptive tracking test for the position reference signal:

$$x_{1d}(t) = 0.3[1 - e^{-2.0t^3} \sin(7t)].$$

The purpose of trying different inputs and angle reference signals is to see the behavior of the schemes in the face of different *excitation* conditions. Also, being aware of the impact the choice of the tuning gains has on the performance of the algorithms, we carry out a discussion on their tuning and show the behavior for various values of these parameters. Unfortunately, as thoroughly discussed in Ortega, Romero & Fang 2025, guidelines for the tuning of SM algorithms are almost always conspicuous by their absence—usually simply saying that the gains have to be taken “*sufficiently*” large.

## 3 Proposed Adaptive Speed Observers and Controllers

In this section we present the mathematical description of the schemes that we will try experimentally as described above. We assume that only the angle  $q$  is measurable and propose to *cancel* the known gravity force, both, in the observers and in the tracking controllers.

Given the *estimated* state vector  $\hat{\mathbf{x}}(t) \in \mathbb{R}^2$ , we denote the state *observation error* as  $\hat{\mathbf{x}} := \hat{\mathbf{x}} - \mathbf{x}$ . On the other hand, for a given position *reference* signal  $x_{1d}(t) \in \mathbb{R}$ , we define the position error  $e_1 := x_1 - x_{1d}$ .

### 3.1 Adaptive speed observers

In this subsection we present the two adaptive speed observers for the system (1).

#### 3.1.1 I&I adaptive observer

The proof of the following proposition may be found in Romero, Ortega, Fang & Bobtsov 2025, Proposition 1.<sup>1</sup>

**Proposition 1** Consider the system (1), assuming that  $u$  ensures the states remain bounded. The I&I adaptive velocity observer:

$$\begin{aligned} \dot{x}_{2I} &= \frac{1}{J}u - \frac{ml_bg}{J} \sin(x_1) - \frac{1}{J}(\hat{\theta}_1 + k_1)\hat{x}_2 \\ &\quad - \frac{1}{J}\hat{\theta}_2 \tanh(\vartheta\hat{x}_2), \end{aligned} \quad (2a)$$

$$\dot{\theta}_{1I} = \gamma_1 \frac{\vartheta}{k_1} \hat{x}_2 \left( \frac{k_1}{J} \hat{x}_2 + \dot{x}_{2I} \right), \quad (2b)$$

$$\dot{\theta}_{2I} = \gamma_2 \frac{\vartheta}{k_1} \tanh(\vartheta\hat{x}_2) \left( \frac{k_1}{J} \hat{x}_2 + \dot{x}_{2I} \right), \quad (2c)$$

with the estimated velocity and parameters given by

$$\hat{x}_2 = x_{2I} + \frac{k_1}{J}x_1, \quad (3a)$$

$$\hat{\theta}_1 = \theta_{1I} - \gamma_1 \frac{\vartheta}{2k_1} \hat{x}_2^2, \quad (3b)$$

$$\hat{\theta}_2 = \theta_{2I} - \gamma_2 \frac{1}{k_1} \ln(\cosh(\vartheta\hat{x}_2)), \quad (3c)$$

and tuning parameters  $k_1, \gamma_1, \gamma_2 > 0$ , guarantees that all signals remain bounded and

$$\lim_{t \rightarrow \infty} [\hat{x}_2(t) - x_2(t)] = 0,$$

for all initial conditions  $(x_1(0), x_2(0), x_{2I}(0), \theta_{1I}(0), \theta_{2I}(0)) \in \mathbb{R}^5$ .  $\square \square \square$

#### 3.1.2 SM adaptive observer

We consider the SM adaptive observer reported in Davila, Fridman & Poznyak 2006, Subsection 6.2, which

<sup>1</sup> In the algorithm given here we have added to extra tuning gains  $\gamma_1, \gamma_2$ , which gives us more flexibility to tune the observer. Their presence does not modify the validity of the convergence claim of Romero, Ortega, Fang & Bobtsov 2025, Proposition 1.

Table 1  
Physical parameters of the pendular device.

| Description                        | Notation   | Value   | Units                         |
|------------------------------------|------------|---------|-------------------------------|
| Length of Link                     | $l$        | 0.313   | m                             |
| Distance to the center of mass     | $l_b$      | 0.0641  | m                             |
| Mass of Link                       | $m$        | 22.4466 | Kg                            |
| Inertia relative to center of mass | $J$        | 0.7013  | Kg m <sup>2</sup>             |
| Viscous friction coefficient       | $\theta_1$ | 5.317   | Nm s/rad                      |
| Coulomb friction coefficient       | $\theta_2$ | 11.6403 | Nm                            |
| Gravity acceleration constant      | $g$        | 9.81    | $\frac{\text{m}}{\text{s}^2}$ |

is given by:

$$\dot{\tilde{x}}_1(t) = \hat{x}_2 + \alpha_2 \sqrt{|\tilde{x}_1|} \text{sign}(\tilde{x}_1) \quad (4a)$$

$$\begin{aligned} \dot{\tilde{x}}_2(t) = & \frac{1}{J} u - \frac{ml_b g}{J} \sin(x_1) - \frac{\bar{\theta}_1}{J} \hat{x}_2 \\ & - \frac{\bar{\theta}_2}{J} \tanh(\vartheta \hat{x}_2) + \alpha_1 \text{sign}(\tilde{x}_1) \end{aligned} \quad (4b)$$

$$\dot{\hat{\Delta}}_\theta = \Gamma \varphi [-\varphi^\top \hat{\Delta}_\theta + \alpha_1 \text{sign}(\tilde{x}_1)] \quad (4c)$$

$$\dot{\Gamma} = -\Gamma \varphi \varphi^\top \Gamma, \quad (4d)$$

where  $\bar{\theta} \in \mathbb{R}^2$  denotes an *a-priori* fixed estimate of the parameters  $\theta$ , the constants  $\alpha_1, \alpha_2$  are positive tuning gains, the regressor vector and the estimated parameters are defined as

$$\varphi := - \begin{bmatrix} \hat{x}_2 \\ \tanh(\vartheta \hat{x}_2) \end{bmatrix}, \quad \hat{\theta} := J \begin{bmatrix} \hat{\Delta}_\theta + \bar{\theta} \end{bmatrix}.$$

It is claimed in Davila, Fridman & Poznyak 2006 that, if the signal  $\varphi$  satisfies the excitation condition

$$\liminf_{t \rightarrow \infty} \frac{1}{t} \int_0^t \varphi(\sigma) \varphi(\sigma)^\top d\sigma > 0, \quad (5)$$

and the controller gains  $\alpha_1, \alpha_2$  are *sufficiently large* then the SM observer (4) *guarantees*

$$\lim_{t \rightarrow \infty} [\hat{x}_i(t) - x_i(t)] = 0, \quad i = 1, 2.$$

$$\lim_{t \rightarrow \infty} [\hat{\theta}_i(t) - \theta_i(t)] = 0, \quad i = 1, 2.$$

The SM design of (4) belongs to the so-called third generation, according to the classification given in Fridman, Moreno, Bandyopadhyay, Kamal & Chalanga 2015.

### 3.2 Adaptive tracking controller

We aim at achieving a closed-loop dynamics of the form

$$\dot{e}_1 = e_2 + \varepsilon_t, \quad (6)$$

$$\dot{e}_2 = -k_p e_1 - k_v e_2 + \varepsilon_t, \quad (7)$$

where  $e_1 := x_1 - x_{1d}$ ,  $e_2 := x_2 - \dot{x}_{1d}$ ,  $k_p, k_v$  are positive constants and  $\varepsilon_t \in \mathbb{R}$  is a generic symbol for a signal *decaying to zero*. It is easy to see that, if  $x_2$  is *measurable* and the friction parameters are *known*, the ideal control law

$$\begin{aligned} u^* = & \theta_1 x_2 + \theta_2 \tanh(\vartheta x_2) + ml_b g \sin(x_1) \\ & + J(\ddot{x}_{1d} - k_p e_1 - k_v(x_2 - \dot{x}_{1d})), \end{aligned} \quad (8)$$

achieves this objective with  $\varepsilon_t \equiv 0$ . To achieve an implementable control, we propose, for both the I&I and SM controllers, to use the estimated speed and parameters reported by the I&I adaptive observer in Subsubsection 3.1.1—in a certainty-equivalent manner—and those reported by the SM adaptive observer in Subsubsection 3.1.2—again, in a certainty-equivalent manner—in (8), respectively. That is, we propose the adaptive control law:

$$\begin{aligned} u = & \hat{\theta}_1 \hat{x}_2 + \hat{\theta}_2 \tanh(\vartheta \hat{x}_2) + ml_b g \sin(x_1) \\ & + J(\ddot{x}_{1d} - k_p e_1 - k_v(\hat{x}_2 - \dot{x}_{1d})). \end{aligned} \quad (9)$$

It is easy to see that replacing the estimated quantities  $(\cdot)$  by  $(\cdot) + (\cdot)$  we obtain  $u = u^* + \varepsilon_t$ , where

$$\begin{aligned} \varepsilon_t = & \theta_1 \tilde{x}_2 + \tilde{\theta}_1 (x_2 + \tilde{x}_2) + \tilde{\theta}_2 \tanh(\vartheta (x_2 + \tilde{x}_2)) \\ & + \theta_2 [\tanh(\vartheta (x_2 + \tilde{x}_2)) - \tanh(\vartheta x_2)] - J k_v \tilde{x}_2. \end{aligned}$$

It is clear from the equation above that, if the estimated parameters  $\hat{\theta}_i$  and estimated velocity  $\hat{x}_2$  converge to their true values, we have that  $\lim_{t \rightarrow \infty} \varepsilon_t(t) = 0$ , thus achieving the control objective, that is, ensuring the closed-loop structure (6)–(7).

It is claimed in Davila, Fridman & Poznyak 2006 that, for the SM scheme discussed in Subsubsection 3.1.2, the convergence required above follows under the standing excitation assumption (5). On the other hand, it is shown in Romero, Ortega, Fang & Bobtsov 2025, Proposition 2, that to ensure parameter convergence in the I&I scheme it is necessary to impose the following

excitation condition.<sup>2</sup>

**Assumption 1** Consider the speed observer of Proposition 1, with the input signal given by (9). Define the vector signal

$$\phi(t) := \begin{bmatrix} \hat{x}_2(t) \\ \tanh(\vartheta \hat{x}_2(t)) \end{bmatrix}. \quad (10)$$

The reference signal  $x_d(t)$  is such that the following condition holds true. There exist sequences of positive numbers  $\{t_k\}$ ,  $\{T_k\}$ , and  $\{\lambda_k\}$  such that  $t_{k+1} \geq t_k + T_k$ , for  $k = 1, 2, \dots$ ,  $\inf\{T_k\} > 0$ ,  $\sup\{T_k\} < \infty$ , and

$$\int_{t_k}^{t_k + T_k} \phi(s) \phi^\top(s) ds \geq \lambda_k I_2 \quad (11)$$

where  $\sum_{k=1}^{\infty} \lambda_k^2 = \infty$ .  $\square \square \square$

The proof of the proposition below may be found in Romero, Ortega, Fang & Bobtsov 2025, Proposition 2.

**Proposition 2** Consider the system (1) in closed-loop with the control (9) where the estimated speed  $\hat{x}_2$  and parameters  $\hat{\theta}_i$ ,  $i = 1, 2$ , are generated by the I&I adaptive speed observer of Proposition 1. If **Assumption 1** holds true the *global tracking objective* is achieved. More precisely, we have that  $\lim_{t \rightarrow \infty} \hat{\theta}_i(t) = 0$ ,  $i = 1, 2$ , consequently ensuring

$$\lim_{t \rightarrow \infty} e_i(t) = 0, \quad i = 1, 2.$$

#### 4 Comparative Experiments: Open-loop estimation

In this section we give the experimental results for the I&I and the SM adaptive observers described above when they are operating in *open-loop* for the two input signals given in test **T1** of Subsection 2.2.

For both input signals the initial conditions of the estimators were set to zero. That is, we set  $\hat{x}_2(0) = 0$ ,  $\hat{\theta}_1(0) = 0$ ,  $\hat{\theta}_2(0) = 0$  for the I&I observer and for the SM observer we selected  $\hat{x}_1(0) = 0$ ,  $\hat{x}_2(0) = 0$ ,  $\Gamma(0) = I_{2 \times 2}$  and  $\Delta_\theta(0) = [0 \ 0]^\top$ . Since the SM observer includes some a-priori estimates of the parameters  $\theta$  we tried two different situations, which are described in the text below. Also, we tried different values for the various tuning parameters, explained also below.

<sup>2</sup> As discussed in Barabanov & Ortega 2017 the condition (11) is *strictly weaker* than the usual persistency of excitation assumption. It is also weaker than (5).

#### 4.1 Results of test **T1** for the input $u = 25 \sin(5t)$

In this case the parameter of the  $\tanh(\cdot)$  was set to  $\vartheta = 50$  for both observers. For the I&I observer we set  $k_1 = 1$ ,  $\gamma_1 = 1$ ,  $\gamma_2 = 1$ . These gains were carefully selected according to the tuning guidelines provided in Ortega, Romero & Fang 2025. Since no tuning rules are available for the SM observer gains  $\alpha_1$  and  $\alpha_2$ , we tried only small and large values.

Fig. 3 shows the behavior of the error signals for the I&I observer. The figure shows that the estimate  $\hat{x}_2(t)$  converges very rapidly to a small neighborhood of  $x_2(t)$ . Moreover, as expected from a “non-exciting” input signal, the estimates  $\hat{\theta}_1$  and  $\hat{\theta}_2$  do not converge to their true values  $\theta_1$  and  $\theta_2$ , however they remain sufficiently close to yield a good speed estimate.

For the SM observer we consider two different scenarios. First, the *ideal* situation where the parameters are *almost exactly* known, that is, we select  $\bar{\theta} = [7 \ 15]^\top$ , whereas the real values are  $\theta = [7.5816 \ 16.5981]^\top$ . The tuning gains were set to  $\alpha_1 = 10$  and  $\alpha_2 = 100$ . The results are shown in Fig. 4. As seen from the figure, even though the initial conditions of the estimates are very close to their true values, the parameter estimates do not converge and exhibit a large peak at the beginning. Moreover, the estimate  $\hat{x}_2$  seems to grow *unbounded*. However, extending the length of the simulation as done in Fig. 5, we observe that it does not diverge, but exhibits an *inadmissible oscillatory behavior* in steady-state.

The superiority of the I&I observer over the SM one is better appreciated in Fig. 6 where the *actual* speed signal is plotted together with its estimate for the I&I and the SM observer, respectively. Notice the large steady-state deviation in the speed estimate of the SM observer.

We then considered the case of the SM observer when the nominal values  $\bar{\theta}$  are *far* from the real ones. Namely, we set  $\bar{\theta} = [0.01 \ 0.01]^\top$ , keeping the same tuning gains  $\alpha_1 = 10$  and  $\alpha_2 = 100$ . The results are shown in Fig. 7. Interestingly, even though the initial parameter estimate is far from their true values, it is seen that the estimates  $\hat{\theta}_1$  and  $\hat{\theta}_2$  behave relatively well, but still do not converge to their real values. Moreover, the initial peaks in the estimated parameters for the case of good and bad knowledge of the parameters are of similar height. This reveals that this term *plays no role* in the observer behavior.

As a final test of the SM observer we tried it with *high tuning gains*  $\alpha_1 = 100$  and  $\alpha_2 = 1000$ , and the *a priori* estimates *very close* to their true value, that is,  $\bar{\theta} = [7 \ 15]^\top$  —with the experimental results given in Fig. 8.

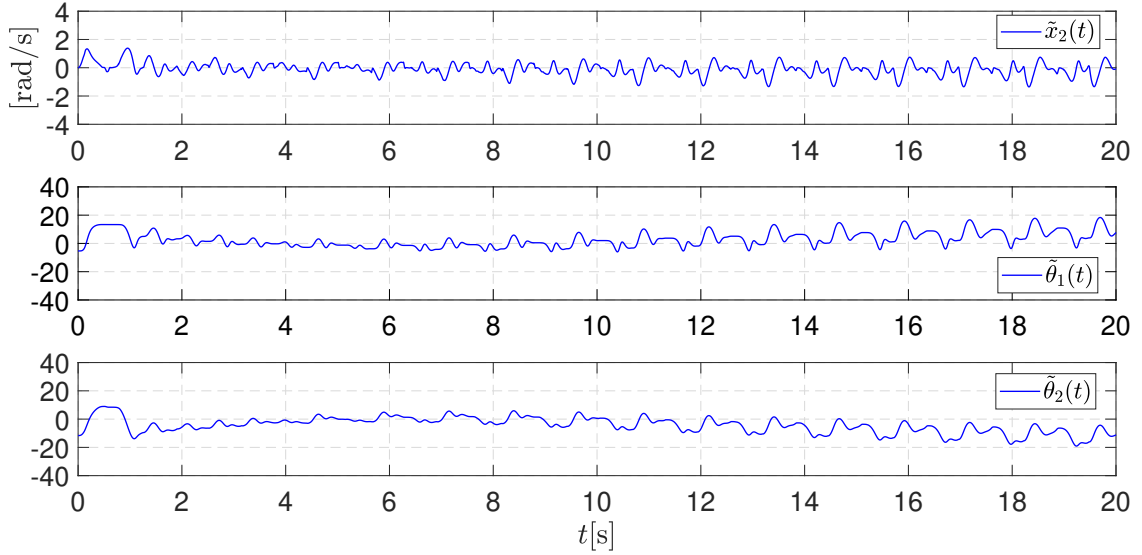


Fig. 3. Behavior of the I&I adaptive observer *error* signals in the open-loop test **T1** for  $u = 25 \sin(5t)$ .

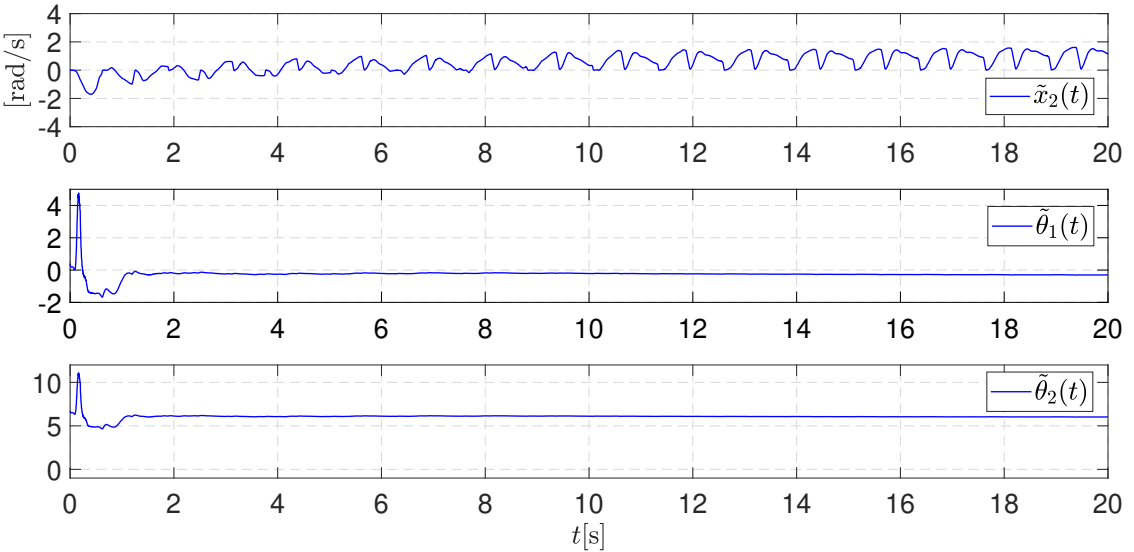


Fig. 4. Behavior of the SM adaptive observer *error* signals in the open-loop test **T1** for  $u = 25 \sin(5t)$  with *excellent* prior knowledge of the parameters.

As seen in the figure, the estimated parameters approximate their true values more closely, showing better behavior than in the other scenarios, but still do not converge, even though their initial values were set closer to the true values.

#### 4.2 Results of test **T1** for the input $u = 14 \operatorname{sign}(\sin(\frac{\pi t}{3}))$

In this case the parameter of the  $\tanh(\cdot)$  was set to  $\vartheta = 500$  for both observers. For the I&I observer we set  $k_1 = 0.7$ ,  $\gamma_1 = 0.7$ ,  $\gamma_2 = 1$  and, similarly to the previous test, all initial conditions were set to zero. For the SM observer

we set the *a priori* estimate of the parameters *almost equal* to their true value, namely,  $\bar{\theta} = [7 \ 15]^\top$ , with the gains  $\alpha_1 = 200$  and  $\alpha_2 = 2000$  and initial conditions  $\hat{x}_1(0) = 0$ ,  $\hat{x}_2(0) = 0$ ,  $\Gamma(0) = 1000I_{2 \times 2}$  and  $\Delta_\theta(0) = [0 \ 0]^\top$ .

Fig. 9 shows the transient behavior of the error signals  $\tilde{x}_2$ ,  $\tilde{\theta}_1$ ,  $\tilde{\theta}_2$  for both observers confirming the superior performance of the I&I one. While the parameter estimate errors of the I&I observer have small oscillations

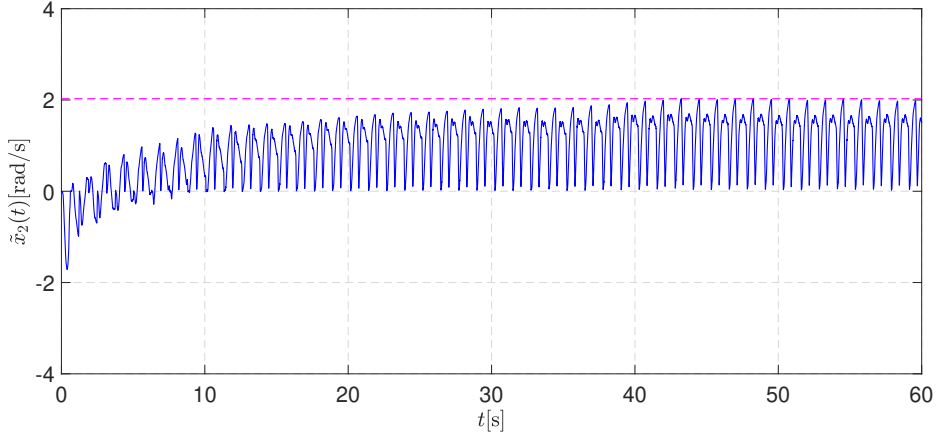


Fig. 5. Speed *error* of SM observer in an extended simulation of Fig. 4.

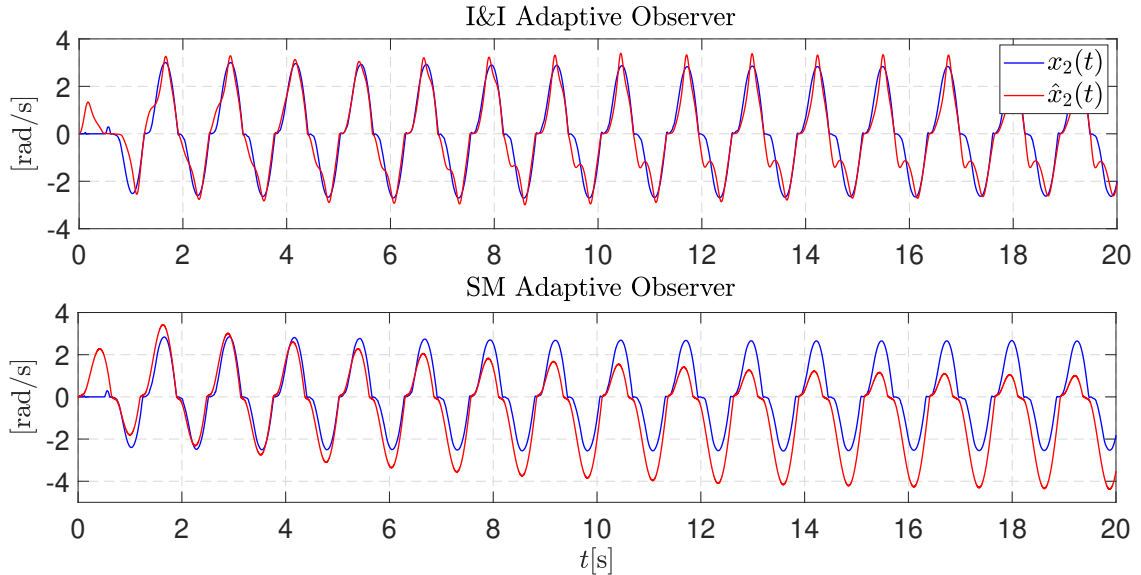


Fig. 6. Behavior of the *actual* and *estimated* velocity of the I&I and the SM adaptive observer in the open-loop test **T1** for  $u = 25 \sin(5t)$ .

around zero, the ones of the SM observer exhibit a very large *steady-state bias*, which seems to be responsible for the poor behavior of the velocity observer. Moreover, as clearly depicted in the zoom of the time window [43, 45] the SM speed estimated has a strong *chattering*.

To further underscore this difference we show in Fig. 10 the *actual* link speed and its estimate for both observers. We bring to your attention the *boxed zooms*, where it is clearly seen that the I&I observers closely tracks  $x_2$ , while the estimate of the SM observers is very far away. It is also noteworthy that the I&I observer signals are *smooth*, in contrast to the SM observer states, particularly the estimate  $\hat{x}_2(t)$ , which exhibits a clear *chattering* effect.

## 5 Comparative Experiments: Adaptive Tracking

The final test was designed to evaluate the performance of the tracking controller discussed in Subsection 3.2, using the I&I and the SM observers. It is proposed that the joint angle  $x_1$  follows the desired trajectory:

$$x_d(t) = 0.3[1 - e^{-2.0t^3} \sin(7t)], \quad (12)$$

which ensures that  $\dot{x}_d(t)$  and  $\ddot{x}_d(t)$  are bounded. The same experiment was also carried out for the “richer” reference signal  $x_d(t) = 0.5 \sin(5t)$ , achieving *better* performance for both observers. In the interest of brevity, we omit the latter results, but they may be found

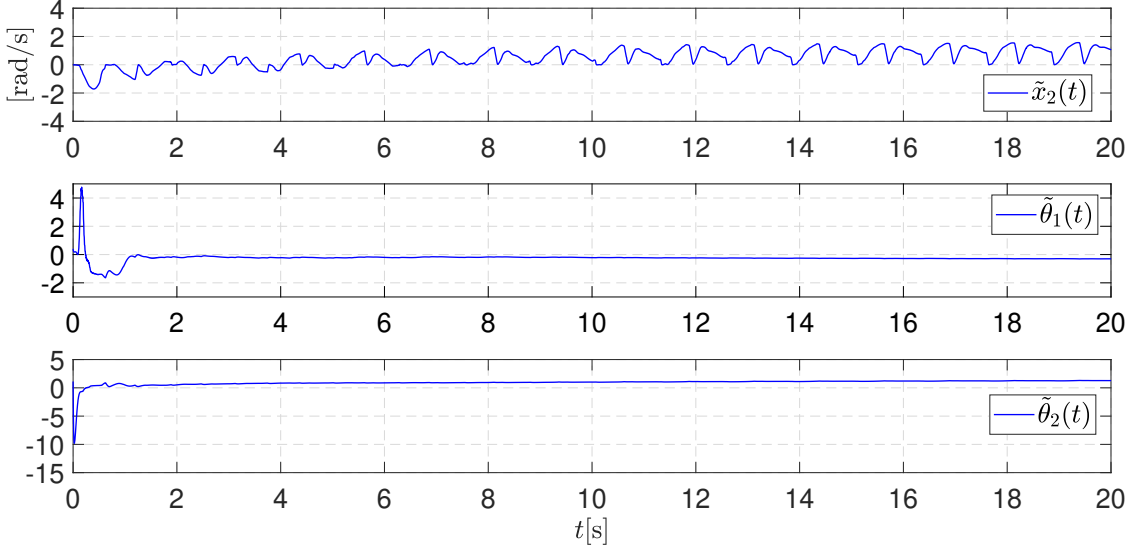


Fig. 7. Behavior of the SM adaptive observer *error* signals in the open-loop test **T1** for  $u = 25 \sin(5t)$  *without* prior knowledge of the parameters.

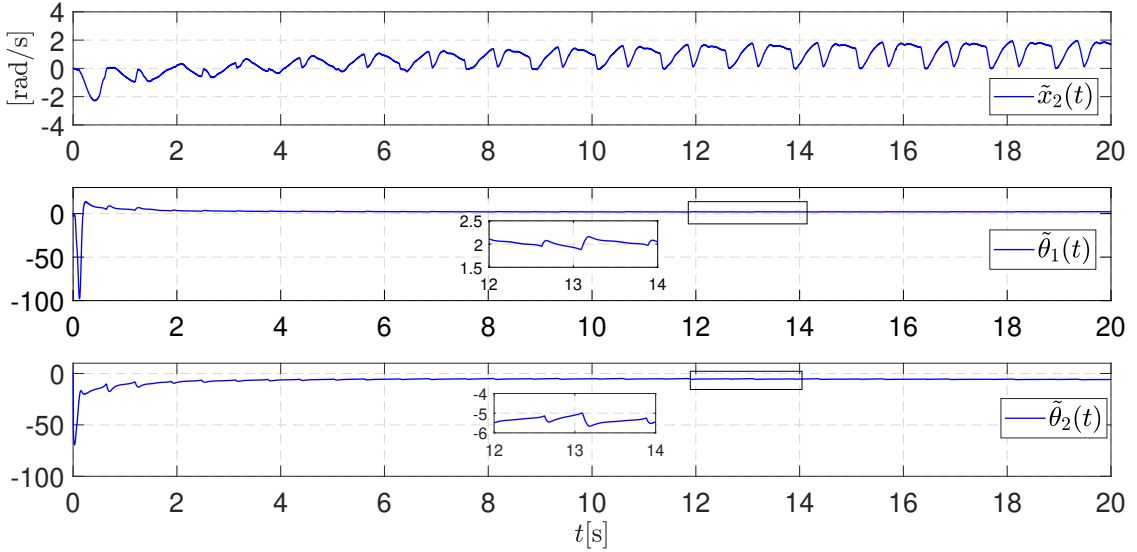


Fig. 8. Behavior of the SM adaptive observer error signals in the open-loop test **T1** for  $u = 25 \sin(5t)$  with *high* gains  $\alpha_1, \alpha_2$ .

in Cervantes-Pérez, Santibáñez, Sandoval, Ortega & Romero 2025.

For these experiments we set the parameter  $\vartheta = 330$  and fix the desired tracking error dynamics via  $k_p = 1600$ ,  $k_v = 1100$ , which corresponds to the poles of the closed loop characteristic polynomial located at  $p_1 = -1.45$  and  $p_2 = -1098.54$ . For the I&I observer we used the gains  $k_1 = 1$ ,  $\gamma_1 = 0.03$ ,  $\gamma_2 = 1$ , and initial conditions  $\hat{x}_2(0) = 0$ ,  $\hat{\theta}_1(0) = 0$ ,  $\hat{\theta}_2(0) = 0$ . The controller gains were selected following the tuning guidelines in Ortega, Romero & Fang 2025. For the SM observer we

used the almost exact parameters  $\bar{\theta} = [7 \ 15]^\top$  and initial conditions  $\hat{x}_1(0) = 0$ ,  $\hat{x}_2(0) = 0$ ,  $\Gamma(0) = 100I_2$ , and  $\Delta\theta(0) = [0 \ 0]^\top$  and set the gains  $\alpha_1 = 100$  and  $\alpha_2 = 1500$ .

Fig. 11 shows the transient behavior of the *estimation error* signals, in Fig. 12 we plot the *actual and estimated* speeds and in Fig. 13 we show the *tracking error* signal for both observers. These figures clearly show the excellent behavior of the I&I scheme. On the other hand, they

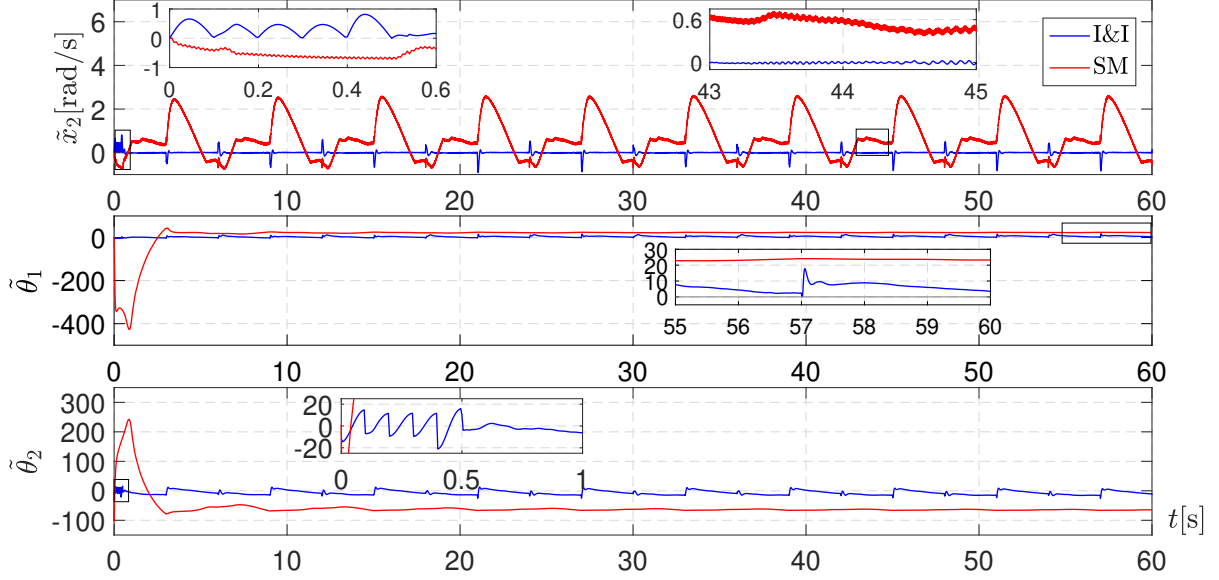


Fig. 9. Behavior of *error* signals in the open-loop test **T1** for  $u = 14 \operatorname{sign}(\sin(\frac{\pi t}{3}))$  for both observers, with *excellent* prior knowledge of the parameters in the SM one.

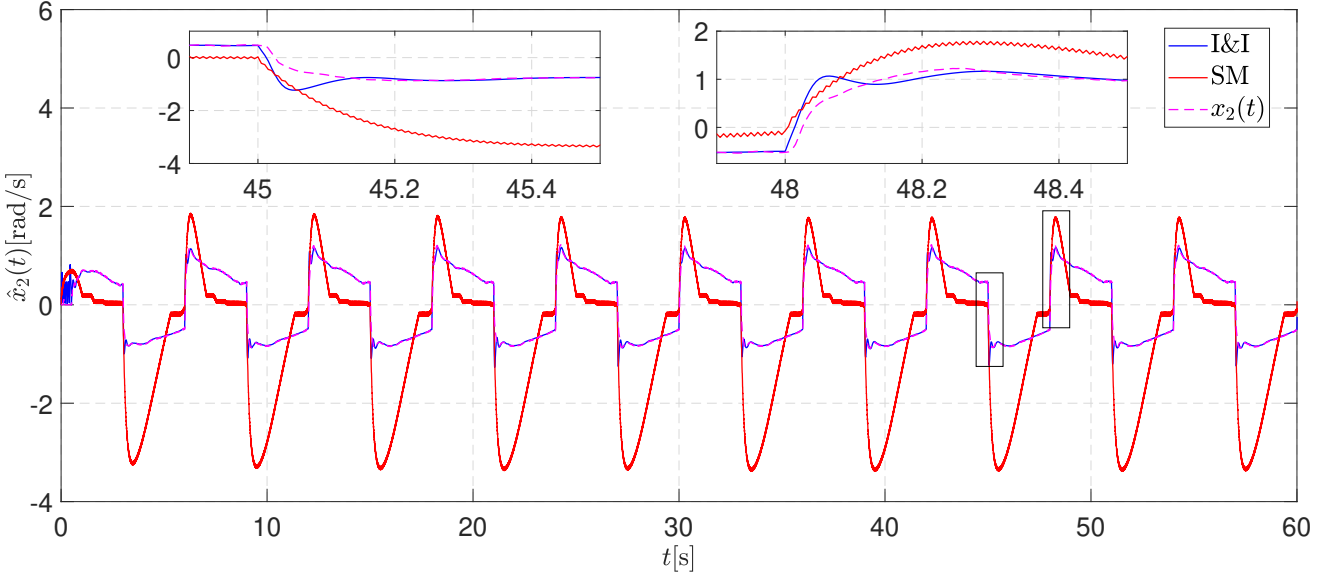


Fig. 10. Behavior of the *actual* joint speed and its estimated values in the open-loop test **T1** for  $u = 14 \operatorname{sign}(\sin(\frac{\pi t}{3}))$  for both observers, with *excellent* prior knowledge of the parameters in the SM one.

reveal the inadmissible performance of the SM one—unquestionably validating our claim of practical inadequacy of this technique.

To further illustrate the deleterious effect of the HG injection implicit in SM designs, we plot the *control* signals for the I&I and SM controllers in Figs. 14 and 15, respectively. While the former exhibits a smooth behavior, the SM control plot shows a high-frequency component, inevitable in HG designs. It was observed that this chattering phenomenon had the pernicious effect of

heating the motor, that was sometimes stopped by the integrated temperature alarm system.

A *video* of the latter experimental test is available in the following link <https://youtu.be/bj3FBN8FLX4>. The desired reference is an oscillation of approximately  $\pm 15^\circ$  around the downwards position of the pendulum. The video clearly shows that the I&I controller closely, and smoothly, tracks this reference. On the other hand, the SM controller drifts approximately  $30^\circ$  counter-clockwise away from the hanging position. It should be

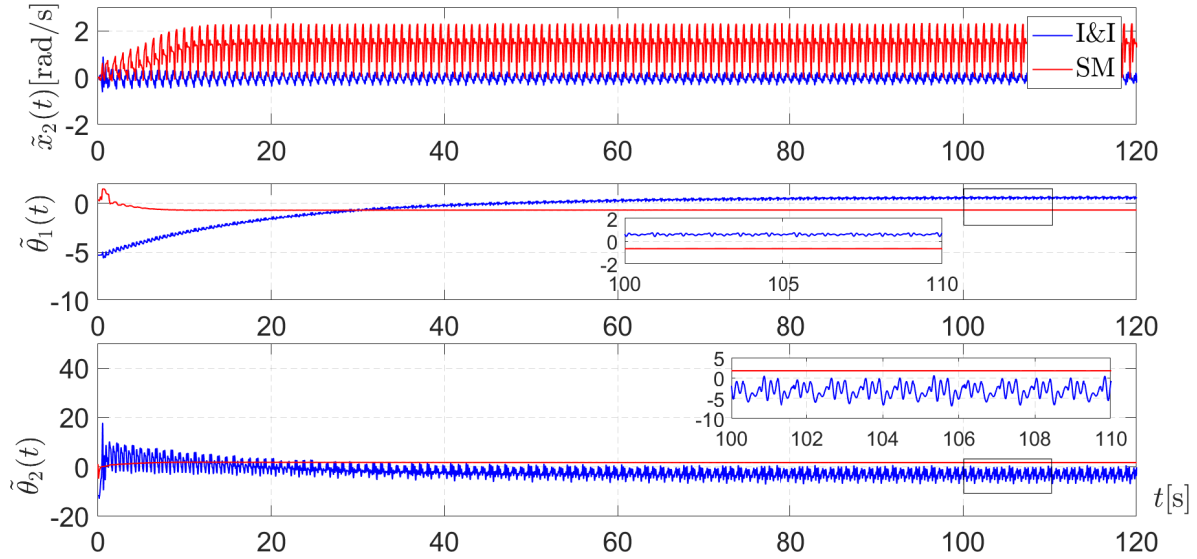


Fig. 11. Behavior of the estimation *error* signals of the I&I and the SM adaptive observers in the trajectory tracking experiment.

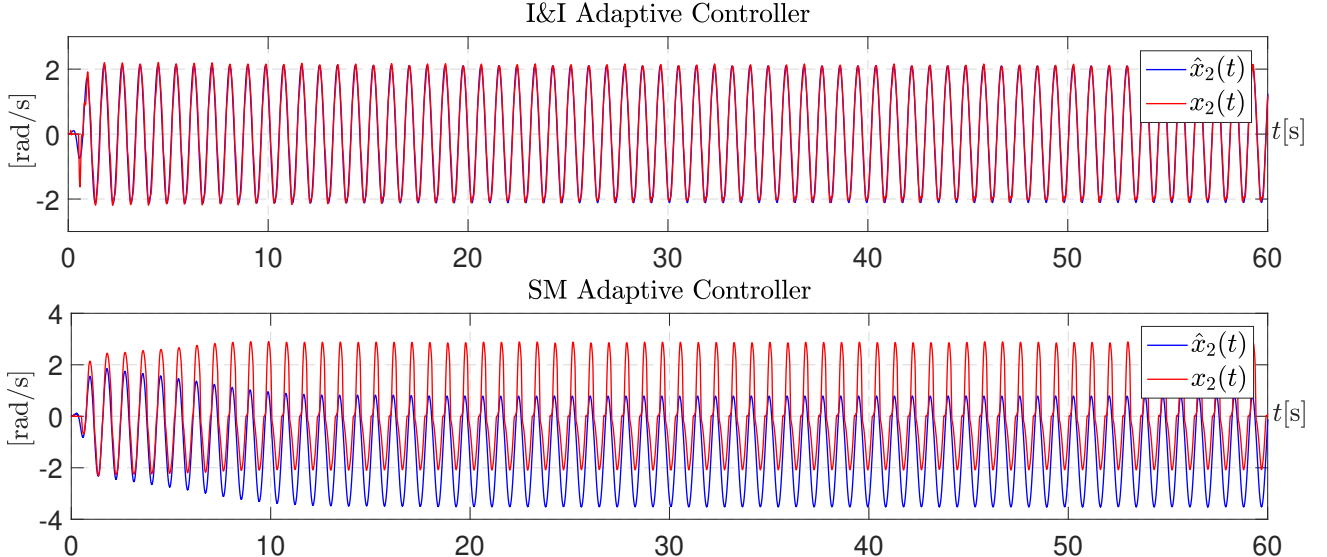


Fig. 12. Behavior of the *actual speed*  $x_2(t)$  and their estimate  $\hat{x}_2(t)$  for the I&I and the SM adaptive observers in the trajectory tracking experiment.

noted also, that the high-frequency components of the control shown in Fig. 15 induce a *motor noise* that is clearly audible in the video.

## 6 The Narrative of Five Generations of SM Controllers

In a recent paper Fridman, Moreno, Bandyopadhyay, Kamal & Chalanga 2015 the authors build up a narrative arguing that SM theory has evolved in five generations. The first one, pioneered by the work of Prof.

Utkin in his ground-breaking 1981 monograph, where the controller is implemented with a *relay* which gives rise to significant chattering and the sliding surface design is restricted to have relative degree one. The second generation starts with the introduction of second order sliding modes, which in the twisting algorithm version boils down to using *two cascaded relay* functions. It is argued that the chattering can be “reduced” adding an integrator in these schemes. The third generation is the super-twisting algorithm that now *splits the two relays* into one acting through the newly added integrator and the other one placed at the level of the control, which is

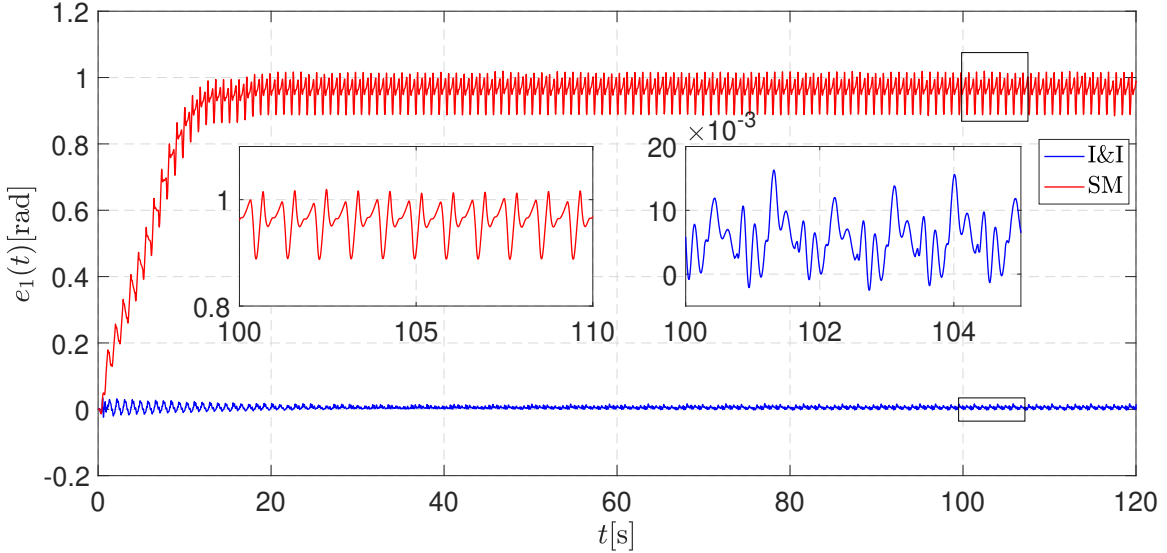


Fig. 13. Behavior of the *tracking error* signal  $e_1(t)$  of the I&I and the SM adaptive controllers in the trajectory tracking experiment.

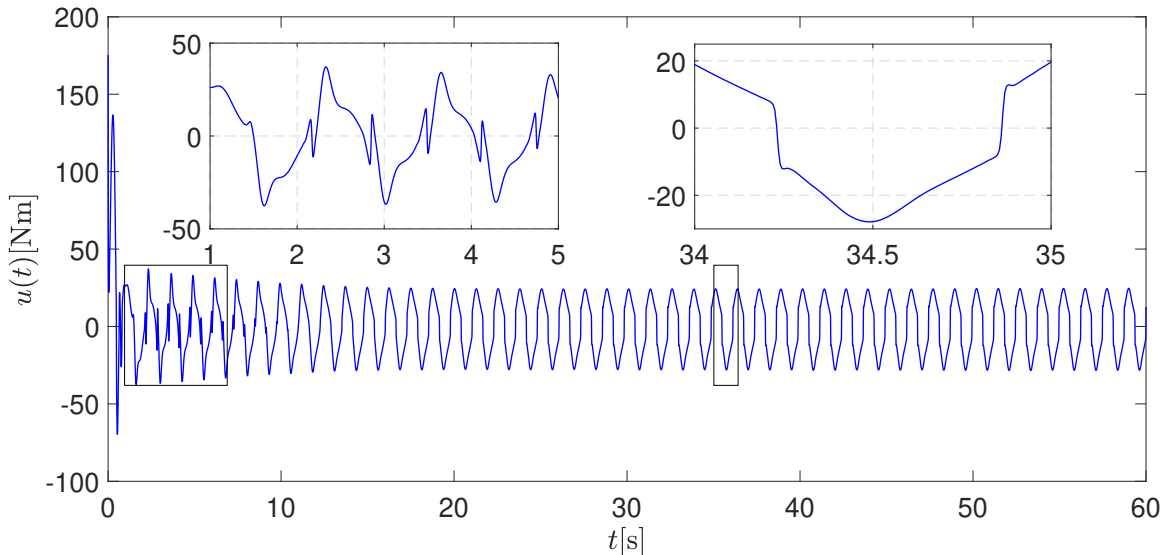


Fig. 14. Behavior of the *control input* of the I&I adaptive controller in the trajectory tracking experiment.

“scaled” with the fractional power of the absolute value of the state. Giving an interpretation of a state observer to this simple structure, it is argued that it can act as a “robust exact SM *differentiator*”. It is recognized that the chattering is not removed with this construction. It is argued that this scheme is insensitive to perturbations with *bounded derivative*—a rather restricted class of perturbations that rules out the typical step disturbance. The fourth generation arrives combining the ubiquitous relay controller with a nested structure of fractional powers of the absolute value of the sliding signal and its successive *derivatives*. The design requires the knowledge of an

upperbound on a high order derivative of the sliding signal, which is not clear where this information will come from. The main objective of the fifth generation SM design is the addition of a *continuity feature*—arguing that due to the latter the chattering will be reduced, but not realizing that the performance degradation comes from the injection of HG through the always present relay operators.

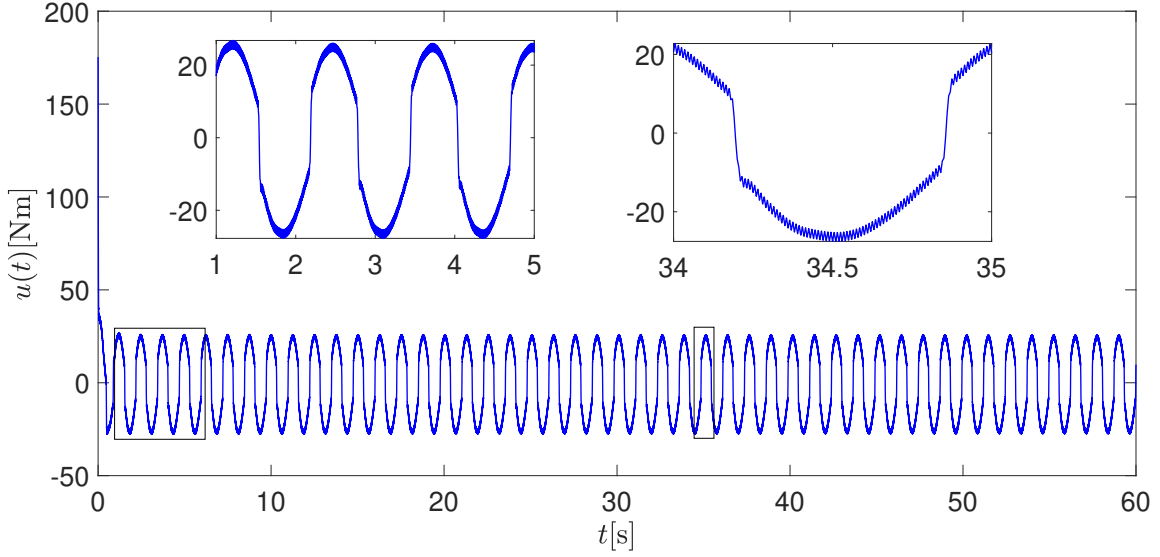


Fig. 15. Behavior of the *control input* of the SM adaptive controller in the trajectory tracking experiment.

### 6.1 Example of a hydro-mechanical system

It may be argued that the newer versions of SM would provide a better performance than the SM design considered in the previous sections pertains to the third generation as per the classification of Fridman, Moreno, Bandyopadhyay, Kamal & Chalanga 2015. To show that the problems highlighted in the experiment prevail in the new generations of SM designs, we present below a simulation study of a fifth generation design recently reported in the literature that clearly validates our argument.

We present in this subsection some simulations of a hydro-mechanical system Pasolli & Ruderman 2018 with the *novel* SM adaptive observer proposed in Estrada, Ruderman, Texis-Loaiza & Fridman 2025. To highlight the performance degradation we compare it with the I&I adaptive observer presented in Romero, Ortega, Fang & Bobtsov 2025. The objective of this study is to confirm that the essential practical limitations of SM designs remain in the newest versions of these schemes.

The dynamic model describing the linearized hydro-mechanical system has the form:

$$\frac{d}{dt} \begin{bmatrix} x_1 \\ x_2 \\ x_3 \end{bmatrix} = \begin{bmatrix} x_2 \\ -\theta_1 x_2 - \theta_2 \tanh(\vartheta x_2) + a_1 x_3 \\ -a_2 x_2 - a_3 x_3 + u \end{bmatrix}, \quad (13)$$

where  $x_1$  and  $x_2$  are the linear displacement and velocity of the cylinder, respectively;  $x_3$  represents the differential load pressure. Following Pasolli & Ruderman 2018

it has been assumed that friction is present in the system modeled by stiction and Coulomb frictions, with  $\theta_1$  and  $\theta_2$  *unknown* parameters and  $a_i, i = 1, \dots, 3$ , and  $\vartheta$  *known* positive constants<sup>3</sup>. In Romero, Ortega, Fang & Bobtsov 2025 an I&I adaptive observer for the system (13) is presented, and its properties are given in the following.

**Proposition 3** Consider the system (13), assuming that  $u$  ensures the states remain bounded. The I&I adaptive velocity observer:

$$\dot{x}_{2I} = a_1 \hat{x}_3 - (\hat{\theta}_1 + k_1) \hat{x}_2 - \hat{\theta}_2 \tanh(\vartheta \hat{x}_2), \quad (14a)$$

$$\dot{\theta}_{1I} = \frac{\vartheta}{k_1} \hat{x}_2 (k_1 \hat{x}_2 + \dot{x}_{2I}), \quad (14b)$$

$$\dot{\theta}_{2I} = \frac{\vartheta}{k_1} \tanh(\vartheta \hat{x}_2) (k_1 \hat{x}_2 + \dot{x}_{2I}), \quad (14c)$$

with the estimated velocity  $\hat{x}_2(t)$ , the estimate  $\hat{x}_3(t)$  of

<sup>3</sup> Note that (13) coincides exactly with the linearized model of Estrada, Ruderman, Texis-Loaiza & Fridman 2025 (equation (6)), being  $a_1 = \frac{A}{m}$ ,  $a_2 = \frac{4EA}{V_t}$ ,  $a_3 = \frac{4EC_{qp}}{V_t}$ ,  $\frac{4EC_q}{V_t} = 1$ ,  $\delta_3(t) = 0$ , and  $F_L(t) = 0$ , where  $E$  is the bulk modulus,  $V_t$  is the total hydraulic volume,  $A$  is the average piston area,  $\delta_3$  is a perturbation in the pressure load, and  $F_L(t)$  represents an external load force. The constants  $C_{qp}$  and  $C_q$  are related to leakage in the cylinder. The function  $\delta_2 := \sigma x_2 - \theta_2 \tanh(\vartheta x_2)$  is defined with  $\theta_2 > 0$ . Thus, it can be defined  $\theta_1 := \sigma(\frac{1}{m} - 1)$ ; provided that  $m < 1$ , then  $\theta_1 > 0$ .

$x_3(t)$ , and the estimated parameters given by

$$\hat{x}_2 = x_{2I} + k_1 x_1, \quad (15a)$$

$$\hat{x}_3 = \int_0^t [-a_2 \hat{x}_2(\tau) - a_3 \hat{x}_3(\tau) + u(\tau)] d\tau, \quad (15b)$$

$$\hat{\theta}_1 = \theta_{1I} - \frac{\vartheta}{2k_1} \hat{x}_2^2, \quad (15c)$$

$$\hat{\theta}_2 = \theta_{2I} - \frac{1}{k_1} \ln(\cosh(\vartheta \hat{x}_2)), \quad (15d)$$

with tuning parameter  $k_1 > 0$ , guarantees that all signals remain bounded and

$$\lim_{t \rightarrow \infty} \begin{bmatrix} \hat{x}_2(t) - x_2(t) \\ \hat{x}_3(t) - x_3(t) \end{bmatrix} = \mathbf{0}_2,$$

for all initial conditions  $(x_1(0), x_2(0), x_{2I}(0), x_3(0), \theta_{1I}(0), \theta_{2I}(0)) \in \mathbb{R}^6$ .  $\square \square \square$

On the other hand, the SM Adaptive obsever of Estrada, Ruderman, Taxis-Loaiza & Fridman 2025 for the system (13) is given by:

$$\dot{\hat{\zeta}}_1 = -L^{\frac{1}{4}} c_1 |\epsilon_1(t)|^{\frac{3}{4}} \text{sign}(\epsilon_1(t)) + \zeta_2, \quad (16a)$$

$$\dot{\hat{\zeta}}_2 = -L^{\frac{2}{4}} c_2 |\epsilon_1(t)|^{\frac{2}{4}} \text{sign}(\epsilon_1(t)) + \zeta_3, \quad (16b)$$

$$\dot{\hat{\zeta}}_3 = -L^{\frac{3}{4}} c_3 |\epsilon_1(t)|^{\frac{1}{4}} \text{sign}(\epsilon_1(t)) + \zeta_4 + a_4 u(t), \quad (16c)$$

$$\dot{\hat{\zeta}}_4 = -L c_4 \text{sign}(\epsilon_1(t)) - a_5 u(t), \quad (16d)$$

where  $a_4$  and  $a_5$  are some given constants stemming from the system model and  $L$  and  $c_i, i = 1, \dots, 4$  are *sufficiently* large gains with  $\epsilon_1 := \hat{\zeta}_1 - x_1$ . Several obscure signal boundedness assumptions on the system signals are then imposed, including the one that the system *acceleration*, as well as the *whole system state are bounded*. Note that the signal  $\hat{\zeta}_2(t)$  represents an estimate of  $x_2(t)$ —that is, the velocity estimate—thus the velocity estimation error can be defined as  $\tilde{\zeta}_2 := \hat{\zeta}_2 - x_2(t)$ . Also note that  $\hat{\zeta}_3(t)$  is an estimate of the time derivative of  $x_2(t)$ , being  $\hat{\zeta}_3(t) = \dot{\hat{\zeta}}_2$ , i.e., the system acceleration; hence,  $\tilde{\zeta}_3 = \hat{\zeta}_3(t) - \zeta_3(t)$  represents the acceleration estimation error. Moreover, in the SM adaptive observer, there is no estimate for the state  $x_3(t)$ , nor for the parameters  $\theta_1$  and  $\theta_2$ . Although it is argued that this technique is “model-based”, this construction does not seem to reflect this claim. Finally, even more distressing condition, is imposed in Assumption 3, where boundedness of the derivative of the input of the tracking error dynamics is supposed. An observer-based controller is also proposed and it is claimed (in Theorem 1), that under the aforementioned boundedness assumptions and a “suitable” selection of two tuning gains, there *exist sufficiently large* values for two more tuning gains that ensures the tracking error goes to zero in “*some*” finite time.

## 6.2 Simulation results

In this subsection we present the results of numerical simulations of the hydro-mechanical system (13) using the I&I adaptive observer (14) and (15) and compare them with the SM adaptive observer (16), using the following input signal:

$$u(t) = 15 \sin(200t). \quad (17)$$

The simulations were carried out in the Matlab/Simulink software using the ODE45 integration method, with an error tolerance of  $1 \times 10^{-6}$ . The nominal dynamic parameters chosen for the hydro-mechanical system (13) were fixed as  $a_1 = 1, a_2 = 1, a_3 = 1$ , that is  $m = 0.5, \sigma = 1, A = 0.5, V_t = 1, E = 0.5, C_q = 0.5, C_{qp} = 0.5$  and  $\theta_1 = 0.01, \theta_2 = 0.01$ , and  $\vartheta = 100$ , while the initial conditions were set as  $[x_1(0) \ x_2(0) \ x_3(0)]^T = [0 \ 0 \ 0]^T$ . For the I&I adaptive observer, we set the initial observer conditions as  $[x_1(0) \ x_2(0) \ x_{2I}(0) \ x_3(0) \ \theta_{1I}(0) \ \theta_{2I}(0)]^T = [0 \ 0 \ 0 \ 0 \ 0 \ 0]^T$  and the gain  $k_1 = 0.005$ . For the SM adaptive observer, we set the initial conditions as  $[\zeta_1(0) \ \zeta_2(0) \ \zeta_3(0) \ \zeta_4(0)]^T = [0 \ 0 \ 0 \ 0]^T$ .

The first simulation test was employed to tune the SM adaptive observer gains. Since, as usual, there is no clear guideline to tune the  $L$  and  $c_i$  observer gains, we selected as an initial point the gains reported in Estrada, Ruderman, Taxis-Loaiza & Fridman 2025, that is,  $L = 650, c_1 = 3, c_2 = 4.16, c_3 = 3.06, c_4 = 1.1$ . However, when running the simulation, *unbounded* trajectories were observed, indicating that the parameter  $c_4$  was too high. Therefore, we decreased it significantly to  $c_4 = 1.1 \times 10^{-4}$ . The results are shown in Fig. 16, which shows that, the velocity estimation for the SM adaptive observer has a good performance; however, chattering appears in the signal  $\tilde{\zeta}_3 = \hat{\zeta}_3 - \zeta_3$ . As explained before, this signal can be seen as an approximation of  $\dot{x}_2(t)$  and is expected to tend to zero in finite time.

Once both observers were tuned, we proceeded with the second simulation, whose purpose was to evaluate the performance of both adaptive observers—after gain tuning—under noise in the measurement of the plant states. Specifically, zero-mean Gaussian noise with a variance of  $1 \times 10^{-4}$  was added to the input control channels of  $x_1(t)$ . The results are shown in Fig. 17. In this case, the SM adaptive observer exhibits a very strong chattering in the error  $\tilde{\zeta}_2$  and  $\tilde{\zeta}_3$ , while the I&I adaptive observer has a smooth response. This confirms that the limitations of SM designs remain present, even in their most recent formulations.

## 7 Concluding Remarks

The experimental evidence presented in the paper unquestionably shows the practical implausibility of high-gain injection-based techniques, for which the SM design

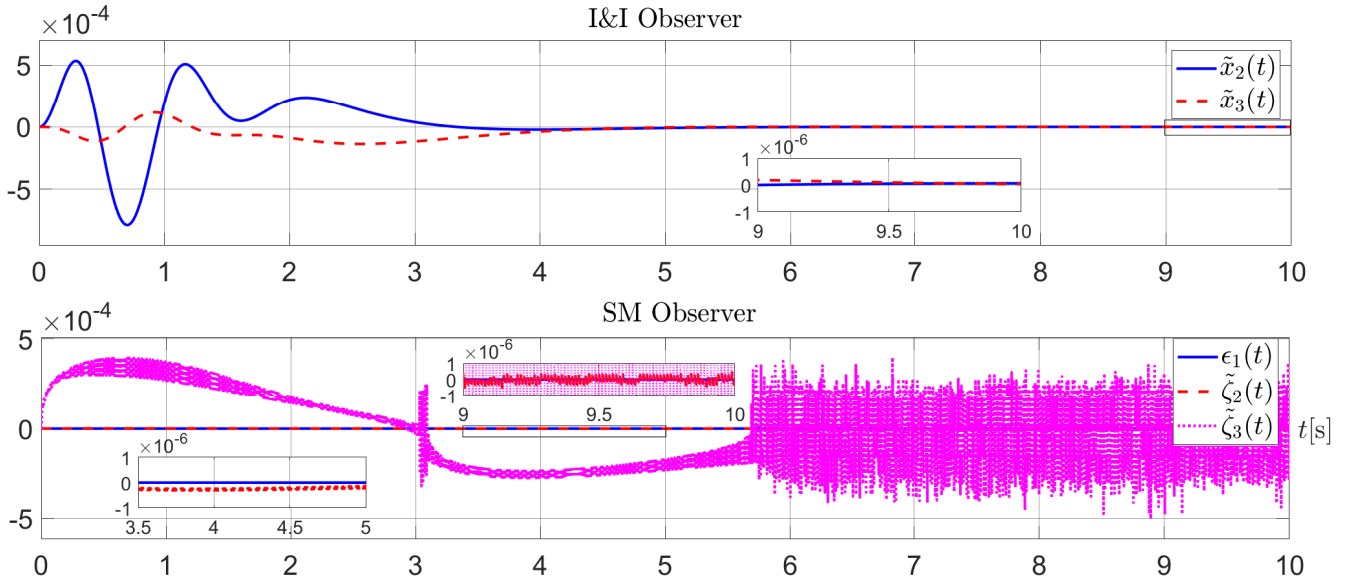


Fig. 16. Behavior of the *error estimates* of the I&I observer and the SM adaptive observer with the hydro-mechanical system (13) in the first simulation.

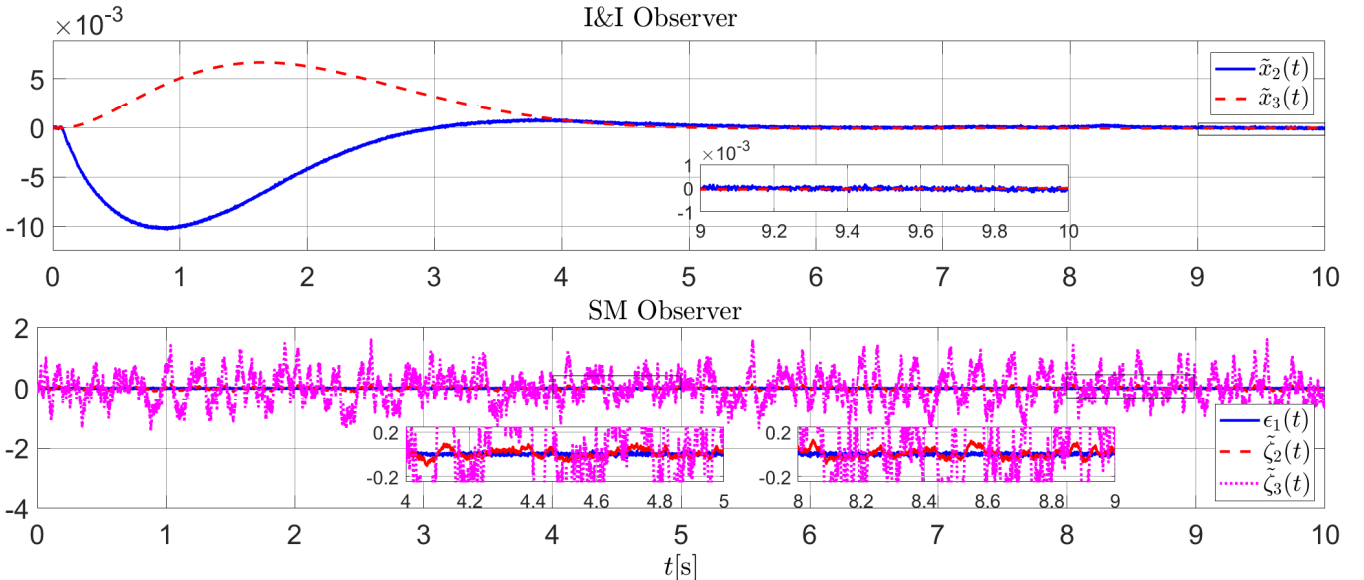


Fig. 17. Behavior of the *error estimates* of the I&I observer and the SM adaptive observer with the hydro-mechanical system (13) in the second simulation.

reported in Davila, Fridman & Poznyak 2006 is a prototypical example. The task that was used to illustrate this fact is the implementation of an adaptive speed observer for the simplest mechanical system—a hanging pendulum—and the associated realization of an adaptive tracking controller. It is shown in Romero, Ortega, Fang & Bobtsov 2025 that this task has a simple solution invoking the well-known I&I theory, a fact that was experimentally verified in this paper. The SM design that was implemented in the experimental facility belongs to the third generation and it may be argued that the newer

versions of SM would provide a better performance. To show that the lack of robustness prevails in the new generations of SM designs, we present a simulation study of a fifth generation design recently reported in the literature that clearly validates our arguments.

We wrap up this paper with a quote from Prof. Utkin's paper Utkin 2016:

*“At the moment the area is not specified where high order SM exhibits efficiency, since serious doubts and counterexamples were demonstrated”.*

## Acknowledgments

This work was partially supported by SECIHTI under Grants CVU 1106239, by TecNM project numbers 22007.25-P, 22483.25-P and by Red Internacional de Control y Cómputo Aplicados del TecNM (RICCA / TecNM).

## Conflict of interest

The authors declare no potential conflict of interests.

## References

Aranovskiy, Stanislav, Romeo Ortega, Jose Guadalupe Romero & Dmitry Sokolov (2019). A Globally Exponentially Stable Speed Observer for a Class of Mechanical Systems: Experimental and Simulation Comparison with High-Gain and Sliding Mode Designs. *International Journal of Control*, 92(7), 1620–1633.

Armstrong-Hélouvy, Brian, Pierre Dupont & Carlos Canudas De Wit (1994). A Survey of Models, Analysis Tools and Compensation Methods for the Control of Machines with Friction. *Automatica*, 30(7), 1083–1138.

Astolfi, Alessandro, Dimitrios Karagiannis & Romeo Ortega (2008). Nonlinear and Adaptive Control With Applications. Springer London.

Barabanov, Nikita & Romeo Ortega (2017). On Global Asymptotic Stability of SPR Adaptive Systems Without Persistent Excitation. *Proceedings of the 56th Annual Conference on Decision and Control (CDC)*, 947–951.

Cervantes-Pérez, Luis, Víctor Santibáñez, Jesús Sandoval, Romeo Ortega & Jose Guadalupe Romero (2025). *Some Reflections on Sliding Mode Designs in Control Systems: An Example of Adaptive Tracking Control for Simple Mechanical Systems with Friction without Measurement of Velocity*, Tech. Rep. Instituto Tecnológico de La Laguna, México.

Davila, Jorge, Leonid Fridman & Alexander Poznyak (2006). Observation and Identification of Mechanical Systems via Second Order Sliding Modes. *Proceedings of the International Workshop on Variable Structure Systems*, 232–237.

Estrada, Manuel A., Michael Ruderman, Oscar Texis-Loaiza & Leonid Fridman (2025). Hydraulic Actuator Control Based on Continuous Higher Order Sliding Modes. *Control Engineering Practice*, 156, 106218.

Fridman, Leonid, Jaime A. Moreno, Bijnan Bandyopadhyay, Shyam Kamal & Asif Chalanga (2015). “Recent Advances in Sliding Modes: From Control to Intelligent Mechatronics”. Springer International Publishing. Chap. Continuous Nested Algorithms : The Fifth Generation of Sliding Mode Controllers, pp. 5–35. ISBN: 978-3-319-18290-2.

Gamez-Herrera, Daniel, Juan Sifuentes-Mijares, Victor Santibáñez & Isaac Gandarilla (2025). Composite Adaptive Control of Robot Manipulators with Friction as Additive Disturbance. *Actuators*, 14(5).

Gandarilla, Isaac, Víctor Santibáñez, Jesús Sandoval & Ricardo Campa (2022). Joint Position Regulation of a Class of Underactuated Mechanical Systems Affected by LuGre Dynamic Friction via the IDA-PBC Method. *International Journal of Control*, 95(6), 1419–1431.

Ortega, Romeo (1982). Experimental Evaluation of Four Microprocessor-Based Advanced Control Algorithms. *Microprocessing and Microprogramming*, 10(4), 229–245.

Ortega, Romeo, Jose Guadalupe Romero & Leyan Fang (2025). Some Reflections on Sliding Mode Designs in Control Systems. *arXiv preprint arXiv:2510.07675*.

Pasolli, Philipp & Michael Ruderman (2018). Linearized Piecewise Affine in Control and States Hydraulic System: Modeling and Identification. *Proceedings of the IECON 2018 - 44th Annual Conference of the IEEE Industrial Electronics Society*, 4537–4544.

Romero, Jose Guadalupe, Romeo Ortega, Leyan Fang & Alexey Bobtsov (2025). Adaptive Compensation of Nonlinear Friction in Mechanical Systems Without Velocity Measurement. *arXiv preprint arXiv:2508.00175*.

Utkin, Vadim (2016). Discussion Aspects of High-Order Sliding Mode Control. *IEEE Transactions on Automatic Control*, 61(3), 829–833.